Received: 8 January 2022 | Revised: 13 June 2022 | Accepted: 20 June 2022
DOI: 10.1002/joc.7769

RESEARCH ARTICLE

International Journal of Climatology RMetS

The observed connection between the Quasi-Biennial Oscillation and the persistence of the North Atlantic Oscillation in boreal winter

Qingyu Cai[1,2] | Tianjiao Ma[1] | Wen Chen[1,2] | Ke Wei[1] | Alexander I. Pogoreltsev[3,4] | Andrey V. Koval[3,4]

[1]Center for Monsoon System Research, Institute of Atmospheric Physics, Chinese Academy of Sciences, Beijing, China
[2]College of Earth and Planetary Sciences, University of Chinese Academy of Sciences, Beijing, China
[3]Saint-Petersburg State University, Saint-Petersburg, Russia
[4]Russian State Hydrometeorological University, Saint-Petersburg, Russia

Correspondence
Tianjiao Ma and Wen Chen, Center for Monsoon System Research, Institute of Atmospheric Physics, Chinese Academy of Sciences, Beijing, China.
Email: matianjiao@mail.iap.ac.cn (T.M.) and cw@post.iap.ac.cn (W.C.)

Funding information
National Natural Science Foundation of China, Grant/Award Numbers: 41975051, 42005032, 42011530082; Russian Foundation for Basic Research, Grant/Award Number: 20-55-53039; China Postdoctoral Science Foundation, Grant/Award Number: 2020M670417

Abstract
This study reveals that the persistence of North Atlantic Oscillation (NAO) during boreal winter is closely linked to the phase of the Quasi-Biennial Oscillation (QBO) at 30 hPa for the period 1958–2020. Our results show that the early winter (i.e., November–December) NAO signal tends to persist into the subsequent January in the easterly phase of the QBO (EQBO). However, in the westerly phase of the QBO (WQBO) there is hardly connection between the early winter and the subsequent January NAO signals. Further analysis suggests that there is stronger stratosphere–troposphere connection and stronger amplitude of the NAO during the early winters of the EQBO compared to those of the WQBO. A stronger NAO in the EQBO tends to induce enhanced positive feedback of air–sea interaction, which may contribute to a prolonged signal of the NAO. Specifically, significant surface heat flux anomalies over the high-latitude and subtropical regions of North Atlantic induced by a stronger early winter NAO may trigger a tripolar pattern of anomalous sea surface temperature in the North Atlantic in the subsequent January. And this anomalous SST pattern may have a feedback on the atmosphere to strength the anomalous NAO by changing the atmospheric baroclinicity and synoptic eddy activities. In contrast, the NAO in the early winters of the WQBO tends to have a weaker amplitude and be confined to the troposphere. This weaker NAO is shown to induce a weaker air–sea interaction in the North Atlantic, and tends not to favour a prolonged NAO.

KEYWORDS
air–sea interaction, North Atlantic, North Atlantic Oscillation, Quasi-Biennial Oscillation, stratosphere–troposphere connection

1 | INTRODUCTION

The North Atlantic Oscillation (NAO) is the dominant mode of the atmospheric variability over the North Atlantic region. It is characterized by a north–south dipole pattern of height anomalies, with one centre located over the Greenland–Iceland region and the other over the mid-latitudes of the North Atlantic (Hurrell, 1995; Hurrell and Van Loon, 1997). Previous studies have documented that the NAO can influence the climate in the North Atlantic coastal regions, such as the North America, the Europe, and the North Africa (Barnston and Livezey, 1987; Rogers, 1997; Wibig, 1999; Wanner *et al.*, 2001; Ning and Bradley, 2016).

The NAO varies at various time scales including intraseasonal and interannual variations (Hurrell and Van Loon, 1997; Wanner *et al.*, 2001). In particular, the NAO exhibits variability of prolonged periods (several months) which may cause persistent climate anomalies. For example, Ogi *et al.* (2003) revealed that summer atmosphere circulation could be influenced by the previous winter NAO, and the external forcing including sea surface temperature (SST) and continental snow cover was suggested to play a key role in connecting the atmospheric internal variability during different seasons. Wu and Chen (2020) presented that the sustained SST anomalies in the North Atlantic facilitated the persistence of the NAO from winter to the subsequent spring. Liu and He (2020) also reported that the NAO in early winter had a delayed effect on European precipitation anomalies in the following February after the late 1980s.

Previous studies have shown that anomalous atmospheric circulation in the stratosphere may have strong impacts on the NAO (e.g., Chen and Zhou, 2012; Kidston *et al.*, 2015; Lu *et al.*, 2020). Baldwin and Dunkerton (1999, 2001) revealed that the stratospheric anomalous Northern Annular Mode (NAM) signal could propagate downward into the troposphere. Ambaum and Hoskins (2002) indicated that the stratosphere potential vorticity (PV) could modulate the height of tropopause and account for part of the NAO variability. Graf and Walter (2005) and Walter and Graf (2005) found that the changes in stratospheric polar vortex could modulate the spatial pattern of the NAO and the associated air–sea coupling processes. Although the mechanisms by which the stratospheric circulation affects the NAO are not fully resolved, some model results have suggested that the prediction skill of the NAO could be improved by considering the stratosphere–troposphere coupling progress (e.g., Scaife *et al.*, 2005; Douville, 2009; Ineson and Scaife, 2009; Nie *et al.*, 2019a; Domeisen *et al.*, 2020).

The Quasi-Biennial Oscillation (QBO) is the dominant mode of the tropical stratospheric variability on interannual time scales, which is characterized by the alternative downward propagation of easterly and westerly winds in the equatorial stratosphere with a period of approximately 28 months (Baldwin *et al.*, 2001; Wei *et al.*, 2007; Rao *et al.*, 2020; Ma *et al.*, 2021; Cai *et al.*, 2022). Although the QBO is a phenomenon in the tropical stratosphere, it can influence climate and weather in the troposphere. In particular, the QBO can cause a NAO-like surface level pressure (SLP) anomaly in the North Atlantic region by affecting the polar vortex in the stratosphere (Baldwin *et al.*, 2001; Marshall and Scaife, 2009; Anstey and Shepherd, 2014; Gray *et al.*, 2018). The stratospheric polar vortex tends to shift toward the Eurasian continent during the easterly QBO phase than that during the westerly QBO phase (Zhang *et al.*, 2019). The QBO could also be associated with the temperature and precipitation anomalies over the Eurasian (Liang *et al.*, 2012; Xue *et al.*, 2015; Song and Wu, 2020).

Previous studies mainly focused on the modulation of the QBO on the phase of the NAO. However, it seems that there is no study to examine the connection between the QBO and the persistence of the NAO so far. In this study, we will show that the early winter (i.e., November–December) NAO signal tends to persist into the following January in the easterly phase of the QBO (EQBO) than in the westerly phase of the QBO (WQBO). The rest of this paper is structured as follows. Section 2 describes the datasets and methods. In section 3, the connection between the QBO and the NAO persistence is presented. Possible physical mechanisms are explored in section 4. In section 5, a summary and a concise discussion are provided.

2 | DATA AND METHODS

2.1 | Datasets and indices

In this study, we use the monthly atmospheric variables from the ERA5 reanalysis dataset (Hersbach *et al.*, 2020). We also repeated the analysis using the NCEP-NCAR and JRA55 reanalysis, and the obtained results are highly consistent with those of the ERA5 (figures not shown). The SST variations are monitored using the monthly Hadley Centre Global Sea Surface Temperature (HadSST) data (Rayner *et al.*, 2003). The monthly Niño3.4 index and NAO index are obtained from the National Oceanic and Atmospheric Administration (NOAA) Climate Prediction Center. The Niño3.4 index is defined as the average equatorial SST anomalies over 5°S–5°N, 170°–120°W. The NAO is the leading mode over the North Atlantic region. A strong (weak) NAO is defined if the absolute value of early winter NAO index is larger (less) than 1 standard deviation (*SD*).

The QBO data provided by the Free University of Berlin are used in this study. This dataset is produced by combining the observations from three radiosonde stations near the equator: Canton Island, Gan/Maldives, and Singapore. We employ the definition of the QBO index as the zonal wind at 30 hPa (Andrews *et al.*, 2019; Labe *et al.*, 2019). A WQBO (an EQBO) is identified when the QBO index is larger (less) than zero. If the QBO index changes its sign in a given winter, that winter will not be classified as EQBO or WQBO. During the analysis period (1958–2020), only the 1969 winter has a phase change in the QBO index. It should be noted that in this study we only analyse the winters with neutral El Niño–Southern Oscillation (ENSO) conditions (Table 1) to exclude possible interferences from the ENSO, since the ENSO has impacts on both the stratospheric polar vortex and the tropospheric circulation anomalies over the North Atlantic–European region (Hoskins and Karoly, 1981; Chen *et al.*, 2003; Garfinkel and Hartmann, 2008; Cheung *et al.*, 2012; Jia *et al.*, 2015; Jimenez-Esteve and Domeisen, 2018; Domeisen *et al.*, 2019). The neutral

TABLE 1 Distribution of the WQBO and the EQBO years in the neutral ENSO conditions, total numbers of high solar activity (hs) years and low solar activity (ls) years in each QBO group

	Years	Total numbers of years	
		HS	**LS**
WQBO	1959^{hs}_{weak}; 1961_{str}; 1963^{ls}_{str}; 1966_{weak}; 1971_{weak}; 1977_{weak}; 1978^{hs}_{weak}; 1980^{hs}_{weak}; 1985^{ls}_{weak}; 1987^{ls}_{weak}; 1990^{hs}_{weak}; 1992_{weak}; 2001^{hs}_{weak}; 2004_{weak}; 2008^{ls}_{weak}; 2013_{weak}; 2016^{ls}_{weak}; 2018^{ls}_{weak}	5	6
EQBO	1958^{hs}_{weak}; 1960_{weak}; 1962^{ls}_{str}; 1967^{hs}_{weak}; 1968^{hs}_{str}; 1970_{str}; 1974^{ls}_{weak}; 1976^{ls}_{weak}; 1979^{hs}_{weak}; 1981^{hs}_{weak}; 1983^{ls}_{weak}; 1989^{hs}_{weak}; 1993_{str}; 1995^{ls}_{str}; 1996^{ls}_{str}; 2000^{hs}_{weak}; 2003_{weak}; 2005^{ls}_{weak}; 2011_{str}; 2012_{weak}; 2014_{str}; 2017^{ls}_{weak}	7	8

Note: Superscript of hs (ls) indicates a year with high (low) solar activity. If the early winter averaged sunspot number is larger (less) than 0.5 *SD*, then the year is defined as high (low) solar activity. Subscript of str(weak) indicates a year with the strong (weak) NAO. If the absolute value of early winter averaged NAO index is larger (less) than 1 *SD*, then the year is defined as strong (weak) NAO.

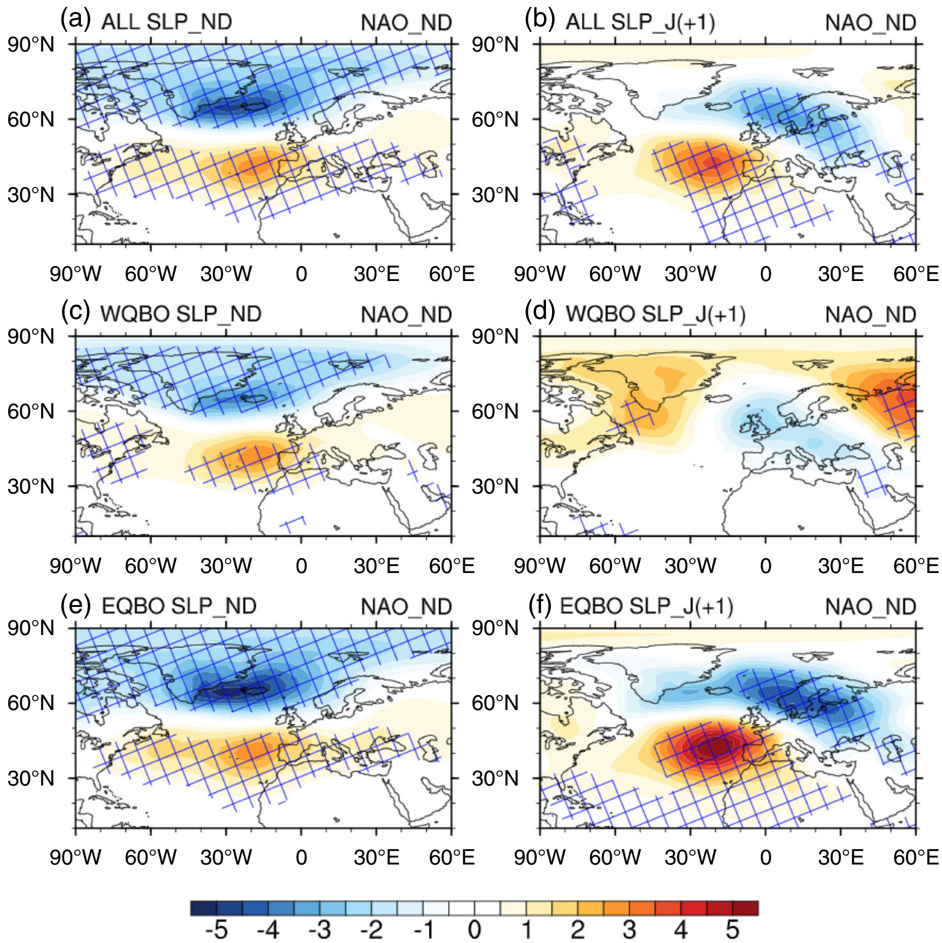

FIGURE 1 Regression patterns of SLP anomalies (shading, unit: hPa) against the normalized early winter NAO index in the simultaneous early winter (a) and the subsequent January (b) for all neutral ENSO years. (c, d) and (e, f) Same as (a, b) but for the WQBO winters and the EQBO winters, respectively. Blue hatched regions indicate anomalies significant at the 90% confidence level [Colour figure can be viewed at wileyonlinelibrary.com]

ENSO winters are identified when the absolute value of the normalized Niño3.4 index is less than 1 *SD* (Nishimoto and Yoden, 2017; Song and Wu, 2020). The present study focuses on the period of 1958–2020 when the QBO data are available. The early winter refers to months of November and December.

Several studies have revealed that the impacts of QBO on the extratropics could be modified by the solar cycle (Labitzke, 1987; Naito and Hirota, 1997). The sunspot number data are used to monitor the solar cycle, which are obtained from the World Center for Sunspot Index and Long-term Solar Observation, Royal Observatory of Belgium, Brussels. A high (low) solar activity year is identified when the early winter averaged sunspot number is larger (less) than 0.5 (−0.5) *SD*. From Table 1, the WQBO and EQBO winters in this study do not have a strong bias against the solar activity.

In order to analyse roles played by the stratospheric process and the North Atlantic SST, the stratospheric polar vortex (SPV) index is defined by using the 50 hPa zonal averaged zonal winds along 60°N. And the North Atlantic tripolar surface net heat flux (NHF) index is defined as the surface net turbulent heat flux anomalies averaged over mid-latitudes North Atlantic (35°–45°N, 45°–35°W) minus the sum of the surface net turbulent heat flux anomalies averaged over North Atlantic subtropics (20°–25°N, 30°–20°W) and high latitudes (55°–65°N, 40°–20°W).

TABLE 2 The correlation coefficients between the early winter (November–December-averaged) NAO indexes and those in the following January during WQBO and EQBO

	Correlation coefficients		
Years	**NAO(ND) and NAO(J + 1)**	**Strong_NAO(ND) and Strong_NAO(J + 1)**	**Weak_NAO(ND) and Weak_NAO(J + 1)**
Total	(40)	(10)	(30)
WQBO	0.15 (18)	(2)	−0.04 (16)
EQBO	0.45* (22)	0.79* (8)	−0.19 (14)

Note: Asterisk (*) indicates that the correlation coefficient exceeds the 95% confidence level. The sample sizes are represented in the brackets.

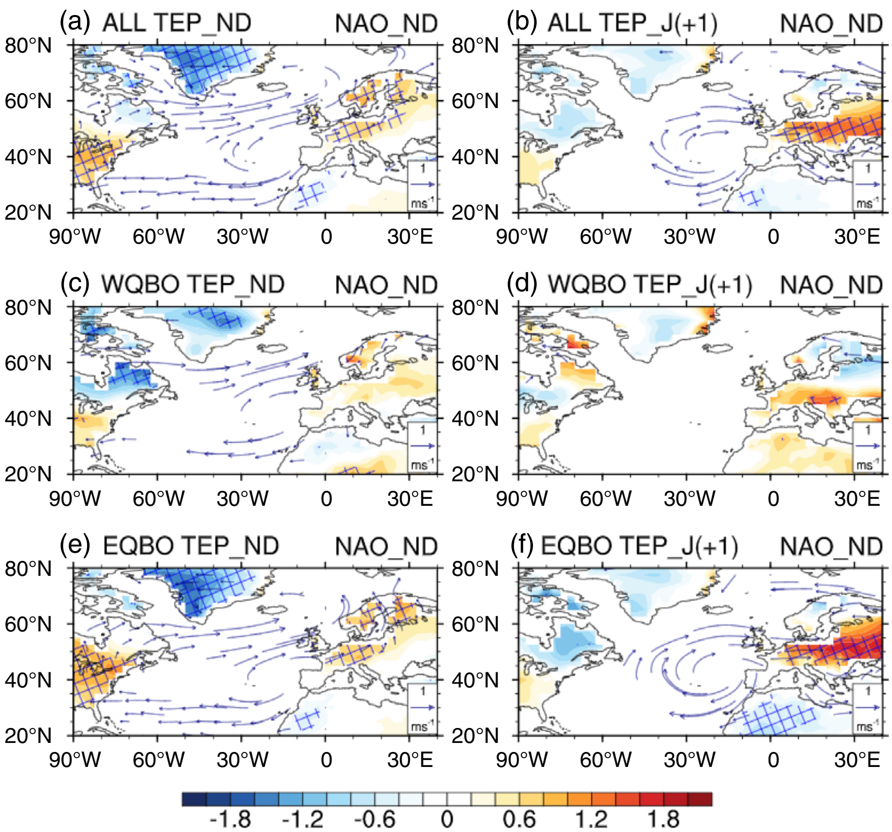

FIGURE 2 Regression patterns of surface temperature anomalies (shading, unit: °C) and surface winds anomalies (vectors, unit: m·s^{-1}) against the normalized early winter NAO index in the simultaneous early winter (a) and the subsequent January (b) for all neutral ENSO years. (c, d) and (e, f) Same as (a, b) but for the WQBO winters and the EQBO winters, respectively. Blue hatched regions indicate anomalies significant at the 90% confidence level. Only anomalous winds that exceed the 90% confidence level are shown as arrows [Colour figure can be viewed at wileyonlinelibrary.com]

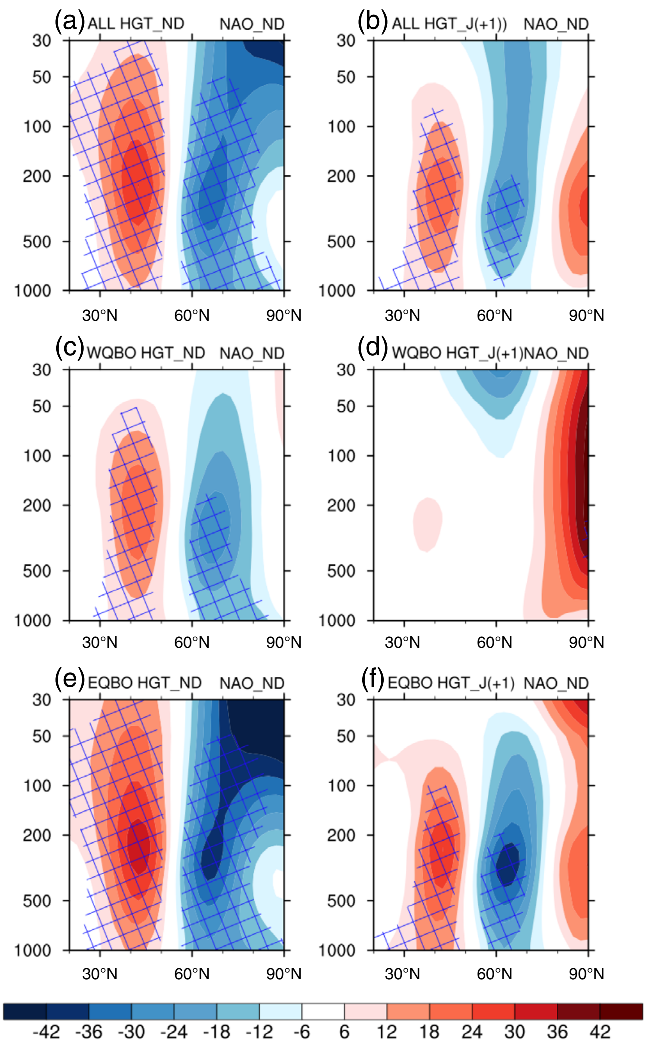

FIGURE 3 Same as in Figure 1, but for the geopotential height anomalies (shading, unit: m) averaged over the North Atlantic for 90°W–30°E [Colour figure can be viewed at wileyonlinelibrary.com]

2.2 | Dynamical diagnostics

2.2.1 | Eady growth rate

The maximum Eady growth rate (EGR) is calculated to measure the atmosphere baroclinicity which follows Vallis (2017):

$$\sigma_{\mathrm{E}} = 0.3098 \frac{|f| \left| \frac{\partial u}{\partial z} \right|}{N}.$$

Here, N is the Brunt–Väisälä frequency, g is the acceleration of gravity, u is the zonal wind, and f is the Coriolis parameter.

2.2.2 | Transient eddy feedback in terms of geopotential tendency

The geopotential height tendency is a quantitative indicator to measure the feedback effect of high frequency transient eddies on the mean flow. The synoptic-scale eddy generated geopotential height tendency can be written as follows (Lau, 1988; Cai *et al.*, 2007):

$$F = \frac{f}{g} \nabla^{-2} \left[-\nabla \cdot \overline{(\boldsymbol{V}' \zeta')} \right],$$

where g and f represent the acceleration of gravity and the Coriolis parameter, respectively. ζ' and $\boldsymbol{V}'$ denote the perturbations of synoptic scale vorticity and horizontal winds. Here, we refer to synoptic scale eddies when atmospheric variables are subjected to a 2–8 day bandpass Lanczos filter (Duchon, 1979).

Active regions of synoptic scale disturbances (known as storm tracks) are located mainly over the North Pacific and the North Atlantic (Blackmon, 1976). Storm tracks can interact with mid-latitude low-frequency atmosphere variability such as the NAO (Limpasuvan and Hartmann, 1999; 2000; Yin, 2005; Riviere and Orlanski, 2007; Luo *et al.*, 2010). In this study, the activity of storm track is represented by the variance of the 2–8 day bandpass filtered 200-hPa geopotential height anomaly (Chen *et al.*, 2020; Ma *et al.*, 2020).

3 | PERSISTENCE OF ANOMALOUS NAO IN DIFFERENT PHASES OF THE QBO

We first revisit the persistence of the anomalous NAO from boreal early winter to the following January. As shown in Figure 1a, the regression pattern of anomalous SLP on the NAO index in early winter is characterized by an enhanced Iceland Low and an enhanced Azores High. This anomalous NAO generally persists into the following January although the Iceland centre is slightly shifted eastward (Figure 1b), which is consistent with previous studies (He *et al.*, 2019; Liu and He, 2020). However, the persistence of anomalous NAO tends to be quite different when the early winters are stratified into the EQBO and WQBO winters. The results indicate that the early winter NAO anomaly can hardly persist into the following January in the WQBO winters (Figure 1c,d). In contrast, Figure 1e,f indicate that the early winter NAO anomaly is more likely to be maintained until the following January in the EQBO winters. Moreover, the spatial pattern of NAO in early winter exhibits different features between the EQBO and WQBO winters (Figure 1c,e).

The northern centre of NAO is stronger in the EQBO than the WQBO winters. And the NAO pattern shows a more latitudinal extension in the EQBO winters compared with the WQBO winters (Figure 1c,e). The above results are robust when we slightly alter the threshold values used to define EQBO and WQBO (figures not shown). The results of correlation analysis are also consistent with the above results (Table 2). The correlation coefficients between the NAO indices in early winter and the following January are 0.45 (exceeding the 95% confidence level) during EQBO and 0.15 (not exceeding the 95% confidence level) during WQBO, respectively. In brief, the QBO may modulate the persistence of the anomalous NAO in boreal early winter with its signal into the subsequent January only in the EQBO.

We next examine the impacts of the early winter NAO on surface air temperature (SAT) over the land of North Atlantic Rim regions during early winter and the subsequent January. Figure 2a shows the conventional regression pattern of SAT onto the NAO index in early winter with cold anomalies over Greenland and North Africa and warm anomalies over the eastern United States and the western Europe. Figure 2b then shows that those anomalies over the western Europe and North Africa tend to persist into the subsequent January. However, the early winter simultaneous SAT anomalies induced by the NAO tend to be much weaker in the WQBO years (Figure 2c) than the EQBO years (Figure 2e). And related to this, the subpolar anomalous cyclone and the anomalous anticyclone over the subtropics tend to be much weaker in the WQBO years (Figure 2c) than the EQBO years (Figure 2e), which induce those SAT anomalies via warm/cold advections. In addition, in the subsequent January, there tends to have hardly any significant SAT anomalies associated with the early winter NAO in the WQBO years (Figure 2d). But in the EQBO years, those SAT anomalies are very significant, especially for the warm anomalies over the western Europe and the cold anomalies over North Africa (Figure 2f). The reason is that there tends to be a much stronger anomalous anticyclone in January

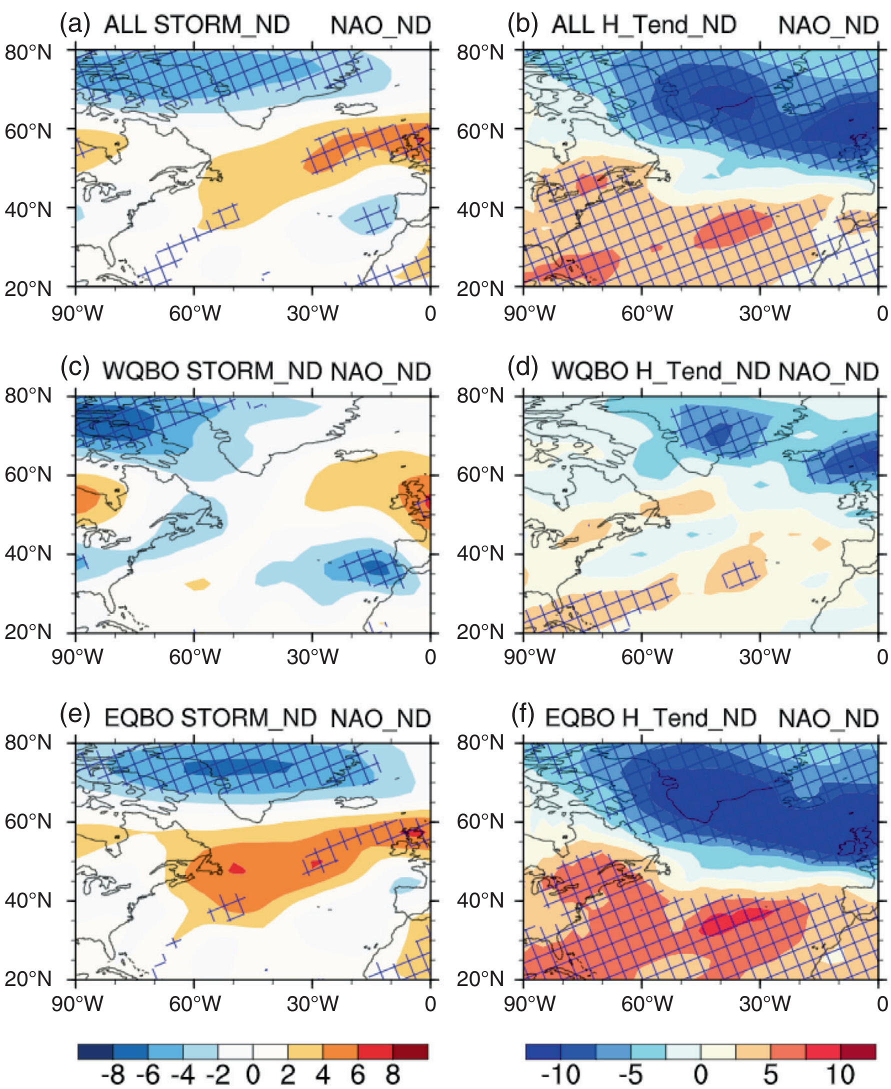

FIGURE 4 Regression patterns of the early winter (a) storm tracks (shading, unit: m) and (b) geopotential height tendency at 300 hPa induced by high-frequency transient eddies (shading, unit: m·day^{-1}) against the simultaneous normalized NAO index for all neutral ENSO years. (c, d) and (e, f) Same as (a, b) but for the WQBO winters and the EQBO winters, respectively. Blue hatched regions indicate anomalies significant at the 90% confidence level [Colour figure can be viewed at wileyonlinelibrary.com]

during EQBO than WQBO (Figure 2d,f), which leads to warm advection to the western Europe and cold advection to the North Africa. Therefore, the persistence of the SAT anomalies associated with the early winter NAO into the subsequent January is predominately in the EQBO winters.

4 | POSSIBLE MECHANISMS

4.1 | Coupling of the NAO with stratosphere in early winter

The amplitude of early winter NAO tends to be larger in the EQBO than the WQBO winters (Figure 1c,e). As shown in Table 2, in the total of 10 strong NAOs, 8 occurred in the EQBO winters and only 2 occurred in the WQBO winters. During the EQBO winters, the correlation coefficient between the early winter strong NAO index and the following January NAO is 0.79 (exceeding the 95% confidence level). However, the relationship between the early winter weak NAO and the following January NAO is weak under both phases of the QBO. Therefore, the larger amplitude of NAO is closely linked with the stronger persistence of the NAO during the EQBO winters. In addition, the amplitude of the NAO may be related to the coupling of the NAO with the stratospheric circulation as suggested by Kuroda (2007). Here we further examine the vertical structure of geopotential height anomalies averaged over the North Atlantic associated with the NAO index in early winter (Figure 3). As shown in Figure 3a, the regression pattern of anomalous geopotential height on the NAO index in early winter is characterized by a meridional dipole nearly in the entire troposphere and stratosphere with increased and decreased height around 40°N and 65°N, respectively. This feature has been referred to the Northern Annular Mode (NAM; Thompson and Wallace, 2000). And this meridional dipole pattern tends to persist into the following January, although its vertical extension becomes

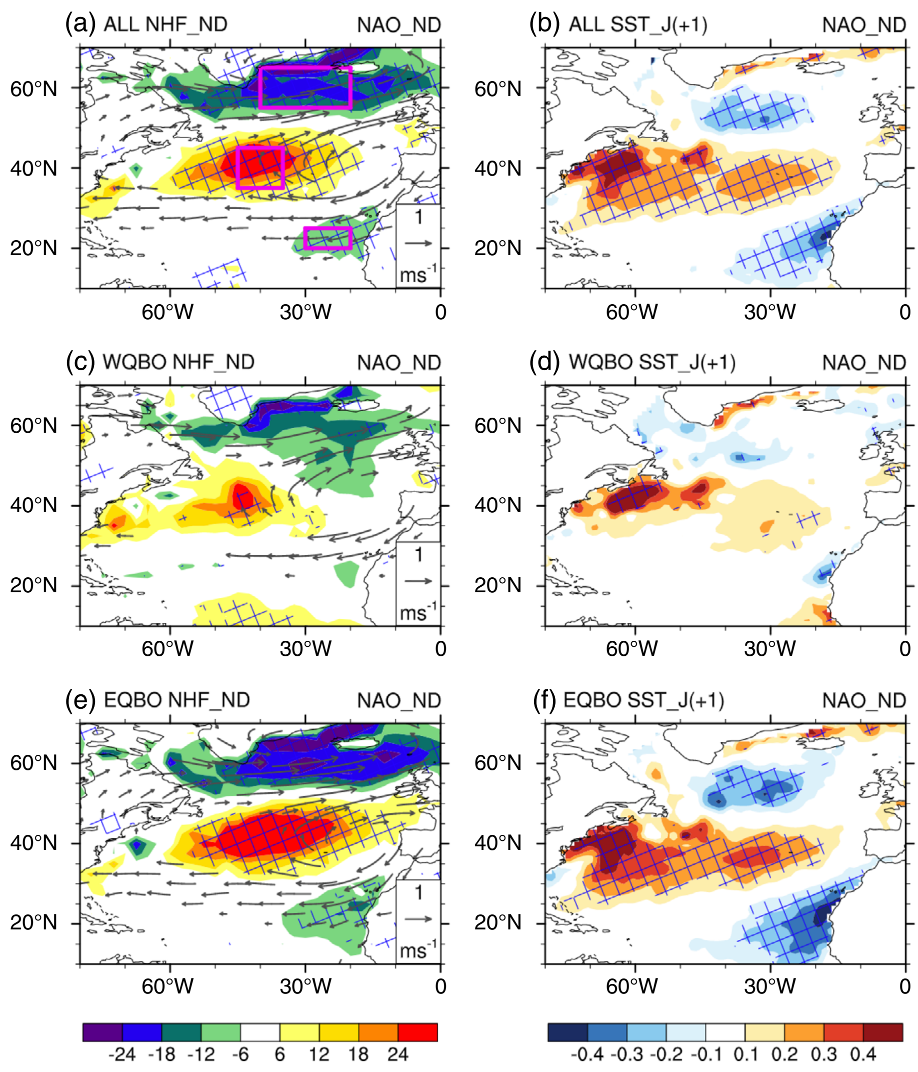

FIGURE 5 Regression patterns of (a) the early winter net turbulent heat flux anomalies (shading, unit: W·m^{-2}) together with surface winds anomalies (vectors, unit: m·s^{-1}) and (b) the SST anomalies (shading, unit: °C) in the subsequent January against the normalized early winter NAO index for all neutral ENSO years. (c, d) and (e, f) Same as (a, b) but for the WQBO winters and the EQBO winters, respectively. Blue hatched regions indicate anomalies significant at the 90% confidence level. Only anomalous winds that exceed the 90% confidence level are shown as arrows. Pink boxes in (a) denote the areas employed to define the early winter NHF index [Colour figure can be viewed at wileyonlinelibrary.com]

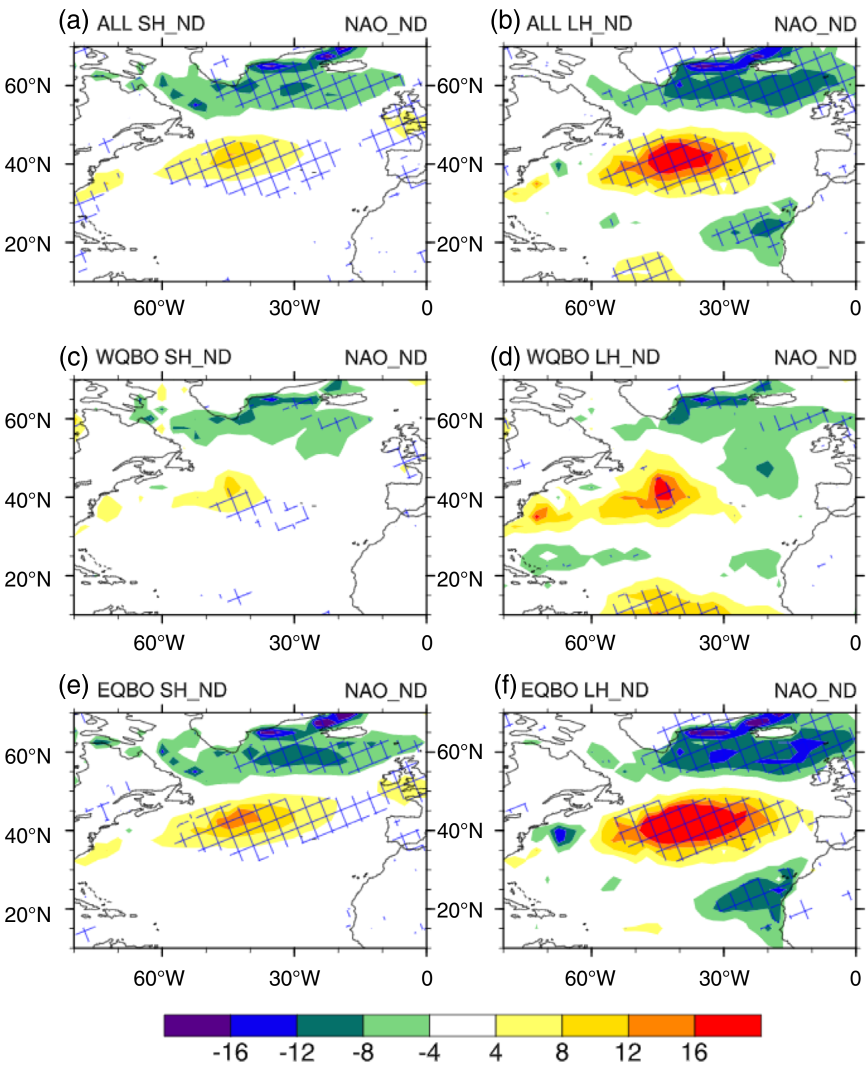

FIGURE 6 Same as in Figure 4, but for the sensible heat net flux anomalies (left; shading, unit: W·m^{-2}) and the latent heat net flux anomalies (right; shading, unit: W·m^{-2}) [Colour figure can be viewed at wileyonlinelibrary.com]

lower (Figure 3b). Further analysis indicates that this anomalous NAM shows different characteristics after the early winters are stratified into the EQBO and WQBO winters. The high-latitude centre of the NAM tends to be mainly confined in the troposphere during WQBO (Figure 3c), and the anomalous NAM's signal nearly disappears in the following January (Figure 3d). In contrast, the vertical structure of the NAM exhibits a stronger connection to the stratosphere and tends to be maintained till the following January during EQBO (Figure 3e,f). Thus, it is suggested that larger amplitude and stronger persistence of the NAO during EQBO may be closely associated with a stronger connection between the tropospheric and the stratospheric circulation.

4.2 | Roles of high-frequency transient eddies in early winter

Previous studies have indicated that the storm track over the North Atlantic can interact with low-frequency atmospheric variability such as the NAO (Limpasuvan and Hartmann, 1999; 2000; Yin, 2005; Riviere and Orlanski, 2007; Luo *et al.*, 2010). Again, we further examine the interaction between the NAO and high-frequency transient eddies as shown in Figure 4a,b. The regressed pattern of storm tracks on the early winter NAO index shows that the high-frequency eddies tend to be decreased over Greenland and increased over the mid-latitudes of North Atlantic, respectively (Figure 4a). These eddy anomalies may in turn lead to the height tendency anomalies similar to a positive NAO pattern (Figure 4b) and thereby enhance the amplitude of NAO variability.

Further comparison of the EQBO with WQBO winters indicates that the early winter NAO tends to be related to a stronger storm track activity during EQBO (Figure 4c,e). And stronger storm track activities may lead to enhanced geopotential height tendency anomalies in the EQBO winters than the WQBO winters (Figure 4d, f). The above results imply a stronger positive feedback between the transient-eddies and the low-frequency NAO during EQBO than WQBO. Thus, the enhanced feedback from the transient eddies may contribute to the larger amplitude of NAO variability in the EQBO winters, too.

4.3 | Roles of the North Atlantic SST anomalies

As an atmospheric internal variability, the NAO is characterized by short memory less than 1 month (Hurrell and Van Loon, 1997; Czaja and Frankignoul, 2002; Ogi *et al.*, 2003). And longer memories of the NAO have been suggested to be related to the SST anomalies with a typical tripolar pattern (Qiao and Feng, 2016; Feng *et al.*, 2018; He *et al.*, 2019). Hence, the changes in North Atlantic SST anomalies in early winter are examined in this study. Figure 5 presents the regression map of surface turbulent heat flux anomalies, surface winds anomalies, and the SST anomalies upon the NAO index during all neutral ENSO years, the EQBO and WQBO years. More specifically, the surface turbulent heat flux anomalies can be decomposed into four components: the surface latent heat flux (LHF), the sensible heat (SHF), the shortwave radiation (SWR), and the longwave radiation (LWR). In response to the anomalous surface winds associated with the NAO, the negative heat flux anomalies are observed over south of the Iceland and the subtropical North Atlantic and the positive heat flux anomalies are observed over mid-latitudes of the North Atlantic (Figure 5a). The positive (negative) net turbulent heat flux anomalies means their directions are downward (upward) and warming (cooling) the local SST. Such tripolar pattern of heat flux anomalies tend to induce a tripolar SST anomalies in the following January (Figure 5b). The surface wind anomalies and corresponding surface turbulent heat flux anomalies associated with the NAO tend to be stronger in the EQBO years (Figure 5e) than the WQBO years (Figure 5c).

Figure 6 shows the LHF and SHF anomalies under different conditions. The anomalous northwesterly winds over the southern Greenland bring colder and dryer Arctic air to the south (Figure 5a), which tend to enhance the difference in temperature and humidity between air and sea surface and induce negative SHF and LHF anomalies in the south of Iceland (Figure 6a,b). And the negative LHF anomalies in the subtropical North Atlantic are induced by the anomalous northeasterly winds via increasing the surface wind velocity (Figure 6b). In addition, anomalous southwesterly winds tend to bring warmer and moister air to the north, which can cause positive SHF and LHF anomalies in the mid-latitudes of the North Atlantic (Figure 6a,b). However, the SHF and LHF anomalies in the regions mentioned above tend to be stronger and more significant during EQBO than those during WQBO. More specifically, there tends to be observed a stronger and wider anomalous SHF over the south of Iceland and mid-latitudes of the North Atlantic and a stronger and clearer tripolar pattern of anomalous LHF over the North Atlantic during EQBO (Figure 6c–f).

To better illustrate the difference in the regression pattern of the net turbulent heat flux under EQBO and WQBO, we further examined the area-averaged regression coefficients in the three areas (the northern

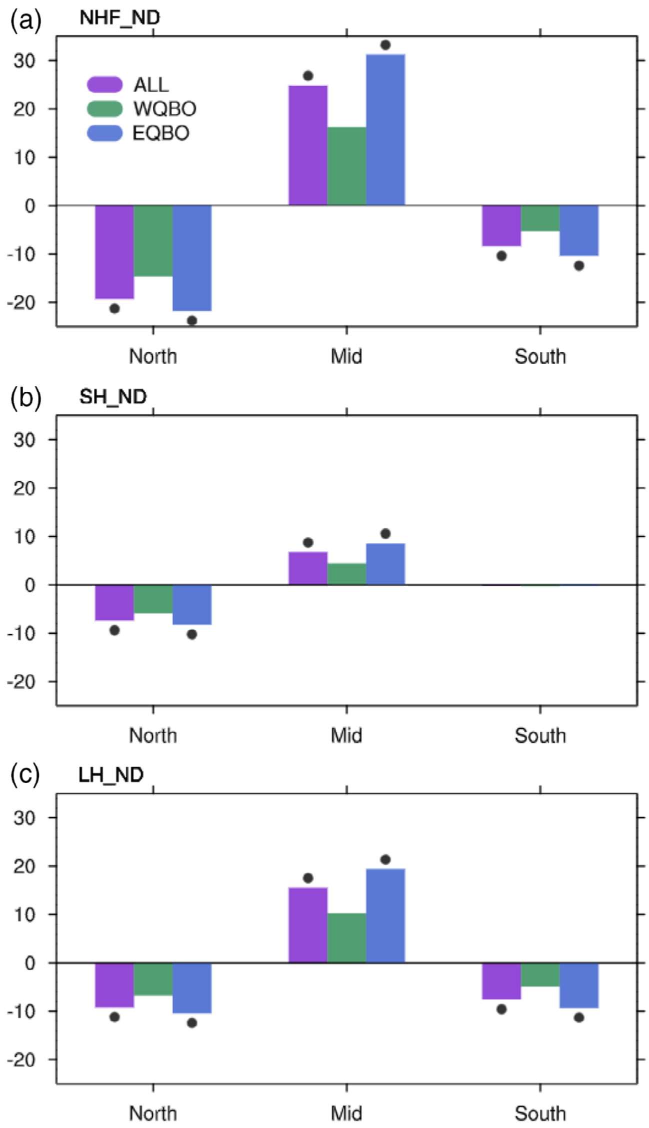

FIGURE 7 Regression coefficients of (a) the early winter net turbulent heat flux anomalies (unit: $W \cdot m^{-2}$) in the northern part (55°–65°N, 40°–20°W), the middle part (35°–45°N, 45°–35°W), and the southern part (20°–25°N, 30°–20°W) of the North Atlantic (i.e., the pink boxes in Figure 5a) against the prior normalized early winter NAO index during the all neutral ENSO (purple), WQBO (green) and EQBO (blue) winters. (b, c) Same as (a) but for the sensible heat net flux anomalies and the latent heat net flux anomalies, respectively. The dots over the bars indicate anomalies at the 90% confidence level [Colour figure can be viewed at wileyonlinelibrary.com]

part: 55°–65°N, 40°–20°W; the middle part: 35°–45°N, 45°–35°W; the southern part: 20°–25°N, 30°–20°W; i.e., the pink boxes in Figure 5a). Figure 7a shows that the net turbulent heat flux anomalies in the three areas are stronger in the EQBO winters than those in the WQBO winters. In addition, the early winter SHF (Figure 7b) and LHF (Figure 7c) anomalies averaged in the three areas are also stronger in the EQBO winters than those in the WQBO winters. In comparison to the SHF and LHF anomalies, the SWR and LWR anomalies associated with the NAO tend to be much weaker in their magnitudes (figures not shown). In other words, the changes in surface turbulent heat flux can be mainly attributed to the SHF and LHF anomalies. Therefore, the stronger North Atlantic SST anomalies during EQBO in January are suggested to be induced mainly by the enhanced SHF and LHF anomalies associated with stronger NAO circulation anomalies in the preceding early winter.

Previous studies have documented that extratropical SST anomalies may change the activity of the transient eddies by modifying the meridional temperature gradient and the atmospheric baroclinicity, and hence further change the feedback effect of transient eddies on the mean flow (Frankignoul, 1985; Kushnir *et al*., 2002; Nie *et al*., 2019b). Figure 5b has shown that the meridional SST gradient in January is increased in the mid-latitudes

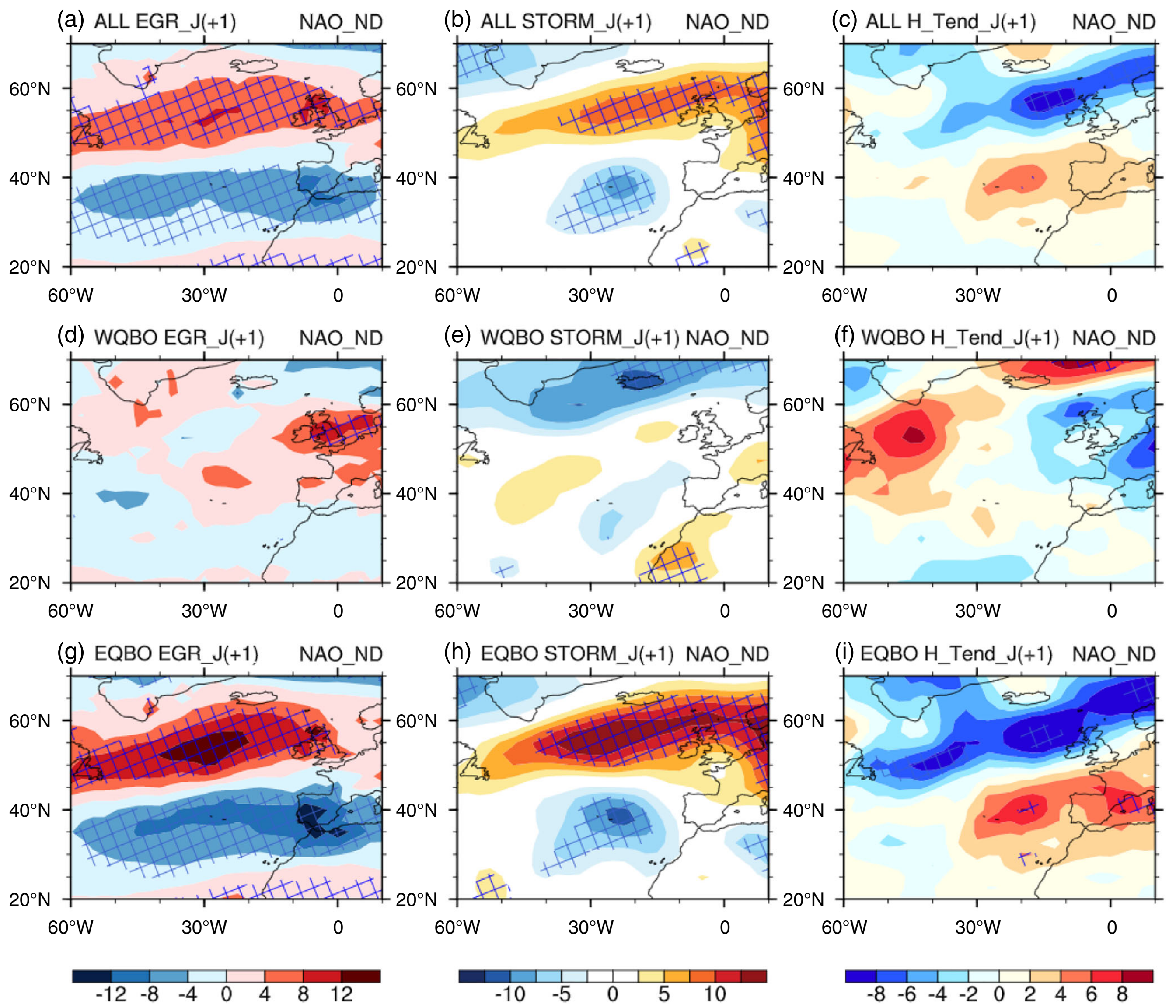

FIGURE 8 Regression patterns against the normalized early winter NAO index for (a) the EGR vertically integrated between 900 and 300 hPa (shading, unit: day^{-1}), (b) the storm tracks (shading, unit: m), and (c) the geopotential height tendency at 300 hPa induced by high-frequency transient eddies (shading, unit: m·day^{-1}) in the subsequent January for all neutral ENSO years. (d–f) and (g–i) Same as (a–c) but for the WQBO winters and the EQBO winters, respectively. Blue hatched regions indicate anomalies significant at the 90% confidence level [Colour figure can be viewed at wileyonlinelibrary.com]

and decreased in the subtropics of the North Atlantic, which is associated with the tripolar SST anomalies induced by the preceding early winter NAO. Hence, we further calculate the EGR, the storm track and the geopotential height tendency associated with the anomalous early winter NAO as shown in Figure 8. The EGR representing the atmosphere baroclinicity tends to be enhanced over the mid-latitude North Atlantic and weakened over the subtropical North Atlantic (Figure 8a). These changes in the EGR generally correspond to a dipole pattern of anomalous storm track activities with positive one over the mid-latitude North Atlantic and negative one over the subtropical North Atlantic (Figure 8b). And the generated geopotential height tendency also exhibits a dipole pattern with negative anomalies over the north and positive anomalies over the south of the North Atlantic, which contributes to a positive NAO in January (Figure 8c). However, when the early winters are stratified into the EQBO and WQBO winters, those dipole patterns in the subsequent January depicted above become more evident and significant during EQBO (Figure 8g–i) but weak and insignificant during WQBO (Figure 8d–f). In brief, during EQBO, early winter NAO tends to have a larger variability and induce stronger SST anomalies via enhanced surface turbulent heat fluxes. And these SST anomalies in the North Atlantic tend to persist into the following January and further have a positive feedback effect on the NAO by modulating the storm track activities. A stronger interaction between atmosphere and ocean is suggested to play a crucial role in the persistence of anomalous NAO from early winter to the following January during EQBO. In contrast, such atmosphere–ocean interaction and eddy feedback effect tend to be fairly weak during WQBO; thus, the early winter NAO anomaly can hardly persist into the following January.

5 | CONCLUSIONS AND DISCUSSIONS

The present study examined the connection between the QBO and the persistence of the NAO during boreal winter by using the observational and reanalysis data for the period 1958–2020. The results indicate that there tends to be a significant (an insignificant) correlation between the NAO in early winter and that in the following January during EQBO (WQBO). In other words, the anomalous NAO in early winter, which is consist of an anomalous cyclone at high-latitude and an anomalous anticyclone at mid-latitude over the North Atlantic, tends to persist into the following January only during the easterly phase of the QBO. In addition, the prolonged climate impacts of the early winter NAO, including the SAT anomalies over the western Europe and North Africa in the subsequent January, are also evident only during EQBO. These SAT anomalies can be attributed to the temperature advection induced by the NAO-related winds anomalies. Specifically, the westerly (northerly) winds along the northern (eastern) flank of the anomalous anticyclone carry warmer (colder) air to the western Europe (North Africa), leading to positive (negative) SAT anomalies over there. The above results suggest that the persistence of the NAO during boreal winter is modified by the QBO in the tropical stratosphere. Given that the QBO could be predicted for more than 3 years in advance (Scaife *et al.*, 2014), the persistence of the NAO may potentially be better predicted if the QBO is taken into account.

Figure 9 illustrates the possible mechanism by which the relationship between the QBO and the persistence of the NAO. A stronger early winter NAO is observed during EQBO than WQBO. The NAO amplitude difference in early winter between EQBO and WQBO is suggested to be attributed from two aspects. One is the difference of stratosphere-troposphere coupling. In the EQBO winters, the early winter NAO presents a quasi-barotropic structure with an extension into the stratosphere. Earlier studies (e.g., Kuroda, 2007) have indicated that the coupling

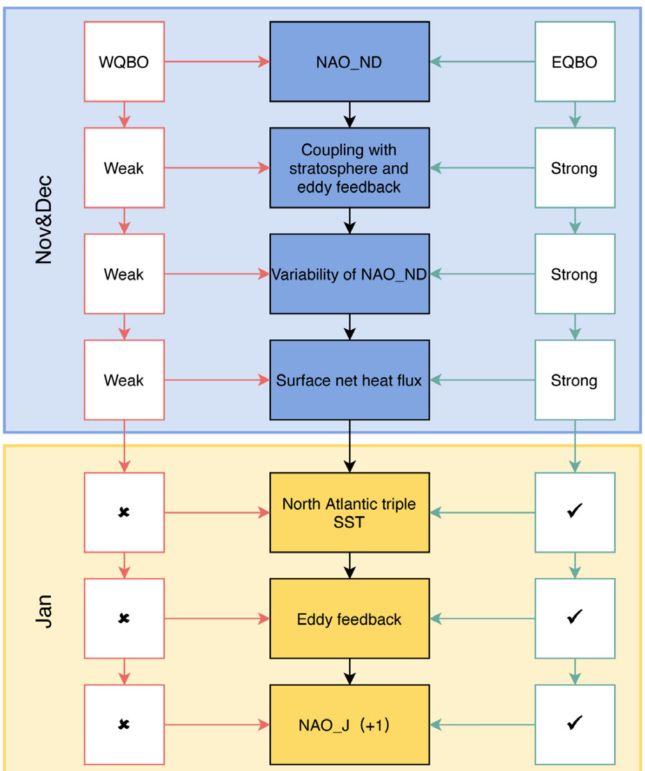

FIGURE 9 Schematic diagram of the physical processes for the QBO to modulate persistence of the NAO [Colour figure can be viewed at wileyonlinelibrary.com]

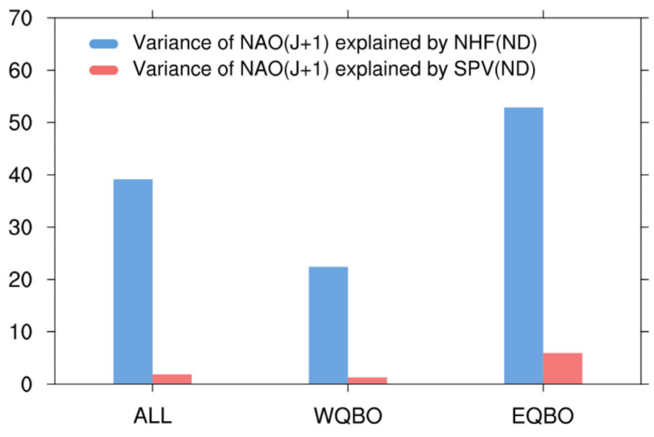

FIGURE 10 The variance of the January NAO index explained by the early winter NHF index (blue bars, unit: %) and SPV index (red bars, unit: %) for all neutral ENSO, WQBO and EQBO winters [Colour figure can be viewed at wileyonlinelibrary.com]

of the NAO with the stratospheric circulation may increase the NAO amplitude in the troposphere. In the WQBO winters, however, the early winter NAO tends to be confined mainly within the troposphere. The other is suggested to be the stronger feedback from high-frequency eddies associated with the NAO during EQBO. Specifically, stronger surface winds anomalies associated with a stronger early winter NAO tend to induce stronger surface heat fluxes, which further lead to a tripolar SST anomaly pattern in the North Atlantic in the following January. And this tripolar SST anomaly pattern may have a positive feedback to the anomalous NAO via changing the atmospheric baroclinicity and the corresponding high-frequency eddy activities. Consequently, the early winter NAO anomaly tends to persist into the subsequent January during EQBO. In contrast, during WQBO, a weaker early winter NAO tends to induce weaker SST anomalies in the North Atlantic, and the associated high-frequency eddies become weaker. Hence, the feedback on the mean atmospheric circulation from eddies are weak and the early winter NAO anomaly can hardly persist into the following January during WQBO.

Previous studies have shown that the coupling between the stratosphere and troposphere is modulated by stratospheric polar vortex (Perlwitz and Graf, 2001; Song and Robinson, 2004; Garfinkel *et al.*, 2013; Xie *et al.*, 2017). A link between the QBO and the intensity of stratosphere-troposphere coupling has been documented. Chen and Li (2007) suggested that the relationship between the East Asian winter SAT anomalies and the stratospheric polar vortex is notable only during the EQBO winters. Kuroda (2007) showed that the NAO and stratosphere flow are closely coupled during the EQBO winters. Zhang *et al.* (2020) found that more negative stratospheric NAM signals extend downward into the troposphere during the EQBO than the WQBO. However, the mechanism by which the dynamical coupling between the stratosphere and troposphere can affect the amplitude of NAO needs to be investigated in the future studies. In addition, the QBO at different levels may have different impacts on the tropospheric circulation (Gray *et al.*, 2018). In this study, the analysis was performed by using the QBO index defined at 30 hPa. We have also examined the results with other QBO indexes at different height levels. For the QBO index at 70 hPa, the results are almost the same as those in this study. However, the persistence of NAO does not exhibit significant difference if using the QBO index at 50 hPa (figures not shown).

Another issue should be addressed is the quantitative contributions to the NAO persistence from the stratospheric process and the feedback between the NAO and SST. Figure 10 presents the variance of the January NAO index explained by the early winter NHF index and SPV index. The early winter NHF can explain 39% of the variance of the following January NAO during neutral ENSO winters. Furthermore, the explained variance by the early winter NHF increases to 53% during the EQBO winters and decreases to 22% during the WQBO winters. In contrast, less than 10% of January NAO variance can be accounted for the early winter SPV under all events. Therefore, a limited direct impact of the SPV on the January NAO is suggested, and the North Atlantic SST anomalies may contribute dominantly to the persistence of the NAO.

ACKNOWLEDGEMENTS

This work was supported jointly by the National Natural Science Foundation of China (Grant Nos. 41975051, 42005032, and 42011530082), the China Postdoctoral Science Foundation (Grant No. 2020M670417), and the Russian Foundation for Basic Research (Grant No. 20-55-53039).

CONFLICT OF INTEREST

The authors declare no potential conflict of interest.

DATA AVAILABILITY STATEMENT

The ERA5 reanalysis dataset are available from European Centre for Medium-Range Weather Forecasts (ECMWF): https://www.ecmwf.int/en/forecasts/datasets/browse-reanalysis-datasets. The monthly Hadley Center Global Sea Surface Temperature (HadSST) data are obtained from: https://www.metoffice.gov.uk/hadobs/hadisst. The QBO data are obtained from the Free University of Berlin on its website: https://www.geo.fu-berlin.de/met/ag/strat/produkte/qbo/qbo.dat. The timeseries of the monthly NAO index and Niño3.4 index are downloaded from the NOAA Climate Prediction Center: https://www.cpc.ncep.noaa.gov/data. The sunspot number data are obtained from http://www.sidc.be/silso/datafiles.

ORCID

Wen Chen https://orcid.org/0000-0001-9327-9079

REFERENCES

Ambaum, M.H.P. and Hoskins, B.J. (2002) The NAO troposphere–stratosphere connection. *Journal of Climate*, 15, 1969–1978. https://doi.org/10.1175/1520-0442.

Andrews, M.B., Knight, J.R., Scaife, A. A., Lu, Y., Wu, T., Gray, L. J. and Schenzinger, V. (2019). Observed and simulated teleconnections between the stratospheric quasi-biennial oscillation and northern hemisphere winter atmospheric circulation. *Journal of Geophysical Research: Atmospheres*, 124(3), 1219–1232. https://doi.org/10.1029/2018jd029368

Anstey, J.A. and Shepherd, T.G. (2014) High-latitude influence of the Quasi-Biennial Oscillation. *Quarterly Journal of the Royal Meteorological Society*, 140, 1–21. https://doi.org/10.1002/qj.2132.

Baldwin, M.P. and Dunkerton, T.J. (1999) Propagation of the Arctic Oscillation from the stratosphere to the troposphere. *Journal of Geophysical Research: Atmospheres*, 104, 30937–30946. https://doi.org/10.1029/1999jd900445.

Baldwin, M.P. and Dunkerton, T.J. (2001) Stratospheric harbingers of anomalous weather regimes. *Science*, 294, 581–584. https://doi.org/10.1126/science.1063315.

Baldwin, M.P., Gray, L.J., Dunkerton, T.J., Hamilton, K., Haynes, P. H., Randel, W.J., Holton, J.R., Alexander, M.J., Hirota, I., Horinouchi, T., Jones, D.B.A., Kinnersley, J.S., Marquardt, C., Sato, K. and Takahashi, M. (2001) The quasi-biennial oscillation. *Reviews of Geophysics*, 39, 179–229. https://doi.org/10.1029/1999rg000073.

Barnston, A.G. and Livezey, R.E. (1987) Classification, seasonality and persistence of low-frequency atmospheric circulation patterns. *Monthly Weather Review*, 115, 1083–1126. https://doi.org/10.1175/1520-0493.

Blackmon, M.L. (1976) Climatological spectral study of 500 mb geopotential height of Northern Hemisphere. *Journal of the Atmospheric Sciences*, 33, 1607–1623. https://doi.org/10.1175/1520-0469.

Cai, M., Yang, S., Van Den Dool, H.M. and Kousky, V.E. (2007) Dynamical implications of the orientation of atmospheric eddies: a local energetics perspective. *Tellus Series A: Dynamic Meteorology and Oceanography*, 59, 127–140. https://doi.org/10.1111/j.1600-0870.2006.00213.x.

Cai, Q., Chen, W., Chen, S., Ma, T. and Garfinkel, C.I. (2022) Influence of the Quasi-Biennial Oscillation on the spatial structure of the wintertime Arctic Oscillation. *Journal of Geophysical Research: Atmospheres*, 127, e2021JD035564. https://doi.org/10.1029/2021JD035564.

Chen, S., Wu, R. and Chen, W. (2020) Strengthened connection between springtime North Atlantic Oscillation and North Atlantic Tripole SST pattern since the late 1980s. *Journal of Climate*, 33, 2007–2022. https://doi.org/10.1175/jcli-d-19-0628.1.

Chen, W. and Li, T. (2007) Modulation of Northern Hemisphere wintertime stationary planetary wave activity: East Asian climate relationships by the Quasi-Biennial Oscillation. *Journal of Geophysical Research: Atmospheres*, 112, 13. https://doi.org/10.1029/2007jd008611.

Chen, W., Takahashi, M. and Graf, H.-F. (2003) Interannual variations of stationary planetary wave activity in the northern winter troposphere and stratosphere and their relations to NAM and SST. *Journal of Geophysical Research: Atmospheres*, 108, 4797. https://doi.org/10.1029/2003JD003834.

Chen, W. and Zhou, Q. (2012) Modulation of the Arctic Oscillation and the East Asian winter climate relationships by the 11-year solar cycle. *Advances in Atmospheric Sciences*, 29(2), 217–226.

Cheung, H.N., Zhou, W., Mok, H.Y. and Wu, M.C. (2012) Relationship between Ural–Siberian blocking and the East Asian winter monsoon in relation to the Arctic Oscillation and the El Niño–Southern Oscillation. *Journal of Climate*, 25, 4242–4257.

Czaja, A. and Frankignoul, C. (2002) Observed impact of Atlantic SST anomalies on the North Atlantic Oscillation. *Journal of Climate*, 15, 606–623. https://doi.org/10.1175/1520-0442.

Domeisen, D.I.V., Butler, A.H., Charlton-Perez, A.J., Ayarzaguena, B., Baldwin, M.P., Dunn-Sigouin, E., Furtado, J. C., Garfinkel, C.I., Hitchcock, P., Karpechko, A.Y., Kim, H., Knight, J., Lang, A.L., Lim, E.-P., Marshall, A., Roff, G., Schwartz, C., Simpson, I.R., Son, S.-W. and Taguchi, M. (2020) The role of the stratosphere in subseasonal to seasonal prediction: 2. Predictability arising from stratosphere–troposphere coupling. *Journal of Geophysical Research: Atmospheres*, 125, e2019JD030923. https://doi.org/10.1029/2019jd030923.

Domeisen, D.I.V., Garfinkel, C.I. and Butler, A.H. (2019) The teleconnection of El Niño–Southern Oscillation to the stratosphere. *Reviews of Geophysics*, 57, 5–47. https://doi.org/10.1029/2018rg000596.

Douville, H. (2009) Stratospheric polar vortex influence on Northern Hemisphere winter climate variability. *Geophysical Research Letters*, 36, L18703. https://doi.org/10.1029/2009gl039334.

Duchon, C.E. (1979) Lanczos filtering in one and 2 dimensions. *Journal of Applied Meteorology*, 18, 1016–1022. https://doi.org/10.1175/1520-0450.

Feng, G.L., Zou, M., Qiao, S.B., Zhi, R. and Gong, Z.Q. (2018) The changing relationship between the December North Atlantic Oscillation and the following February East Asian trough before and after the late 1980s. *Climate Dynamics*, 51, 4229–4242. https://doi.org/10.1007/s00382-018-4165-8.

Frankignoul, C. (1985) Sea-surface temperature anomalies, planetary-waves, and air–sea feedback in the middle latitudes. *Reviews of Geophysics*, 23, 357–390. https://doi.org/10.1029/RG023i004p00357.

Garfinkel, C.I. and Hartmann, D.L. (2008) Different ENSO teleconnections and their effects on the stratospheric polar vortex. *Journal of Geophysical Research: Atmospheres*, 113, 14. https://doi.org/10.1029/2008JD009920.

Garfinkel, C.I., Waugh, D.W. and Gerber, E.P. (2013) The effect of tropospheric jet latitude on coupling between the stratospheric polar vortex and the troposphere. *Journal of Climate*, 26, 2077–2095. https://doi.org/10.1175/Jcli-D-12-00301.1.

Graf, H.F. and Walter, K. (2005) Polar vortex controls coupling of North Atlantic Ocean and atmosphere. *Geophysical Research Letters*, 32, L01704. https://doi.org/10.1029/2004gl020664.

Gray, L.J., Anstey, J.A., Kawatani, Y., Lu, H., Osprey, S. and Schenzinger, V. (2018) Surface impacts of the Quasi Biennial Oscillation. *Atmospheric Chemistry and Physics*, 18, 8227–8247. https://doi.org/10.5194/acp-18-8227-2018.

He, S.P., Wang, H.J., Gao, Y.Q. and Li, F. (2019) Recent intensified impact of December Arctic Oscillation on subsequent January temperature in Eurasia and North Africa. *Climate Dynamics*, 52, 1077–1094. https://doi.org/10.1007/s00382-018-4182-7.

Hersbach, H., Bell, B., Berrisford, P., Hirahara, S., Horanyi, A., Munoz-Sabater, J., Nicolas, J., Peubey, C., Radu, R., Schepers, D., Simmons, A., Soci, C., Abdalla, S., Abellan, X., Balsamo, G., Bechtold, P., Biavati, G., Bidlot, J., Bonavita, M., De Chiara, G., Dahlgren, P., Dee, D., Diamantakis, M., Dragani, R., Flemming, J., Forbes, R., Fuentes, M., Geer, A., Haimberger, L., Healy, S., Hogan, R.J., Hólm, E., Janisková, M., Keeley, S., Laloyaux, P., Lopez, P., Lupu, C., Radnoti, G., de Rosnay, P., Rozum, I., Vamborg, F., Villaume, S. and Thepaut, J.N. (2020) The ERA5 global reanalysis. *Quarterly Journal of the Royal Meteorological Society*, 146, 1999–2049. https://doi.org/10.1002/qj.3803.

Hoskins, B.J. and Karoly, D.J. (1981) The steady linear response of a spherical atmosphere to thermal and orographic forcing. *Journal of the Atmospheric Sciences*, 38, 1179–1196. https://doi.org/10.1175/1520-0469.

Hurrell, J.W. (1995) Decadal trends in the North Atlantic Oscillation: regional temperatures and precipitation. *Science*, 269, 676–679. https://doi.org/10.1126/science.269.5224.676.

Hurrell, J.W. and Van Loon, H. (1997) Decadal variations in climate associated with the North Atlantic Oscillation. *Climatic Change*, 36, 301–326. https://doi.org/10.1023/a:1005314315270.

Ineson, S. and Scaife, A.A. (2009) The role of the stratosphere in the European climate response to El Niño. *Nature Geoscience*, 2, 32–36. https://doi.org/10.1038/ngeo381.

Jia, X.J., Wang, S., Lin, H. and Bao, Q. (2015) A connection between the tropical Pacific Ocean and the winter climate in the Asian-Pacific region. *Journal of Geophysical Research: Atmospheres*, 120, 430–448. https://doi.org/10.1002/2014JD022324.

Jimenez-Esteve, B. and Domeisen, D.I.V. (2018) The tropospheric pathway of the ENSO–North Atlantic teleconnection. *Journal of Climate*, 31, 4563–4584. https://doi.org/10.1175/jcli-d-17-0716.1.

Kidston, J., Scaife, A.A., Hardiman, S.C., Mitchell, D.M., Butchart, N., Baldwin, M.P. and Gray, L.J. (2015) Stratospheric influence on tropospheric jet streams, storm tracks and surface weather. *Nature Geoscience*, 8, 433–440. https://doi.org/10.1038/ngeo2424.

Kuroda, Y. (2007) Effect of QBO and ENSO on the solar cycle modulation of winter North Atlantic Oscillation. *Journal of the Meteorological Society of Japan*, 85, 889–898. https://doi.org/10.2151/jmsj.85.889.

Kushnir, Y., Robinson, W.A., Blade, I., Hall, N.M.J., Peng, S. and Sutton, R. (2002) Atmospheric GCM response to extratropical SST anomalies: synthesis and evaluation. *Journal of Climate*, 15, 2233–2256. https://doi.org/10.1175/1520-0442.

Labe, Z., Peings, Y. and Magnusdottir, G. (2019). The effect of QBO phase on the atmospheric response to projected arctic sea ice loss in early winter. *Geophysical Research Letters*, 46(13), 7663–7671. https://doi.org/10.1029/2019gl083095

Labitzke, K. (1987). Sunspots, the QBO, and the stratospheric temperature in the north polar region. *Geophysical Research Letters*, 14(5), 535–537. https://doi.org/10.1029/gl014i005p00535

Lau, N.C. (1988) Variability of the observed midlatitude storm tracks in relation to low-frequency changes in the circulation pattern. *Journal of the Atmospheric Sciences*, 45, 2718–2743. https://doi.org/10.1175/1520-0469.

Liang, W.L., Jian, M.Q. and Qiao, Y.T. (2012) Relationship between QBO and the onset of South China Sea summer monsoon. *Journal of Tropical Meteorology*, 29, 910–942 (in Chinese).

Limpasuvan, V. and Hartmann, D.L. (1999) Eddies and the annular modes of climate variability. *Geophysical Research Letters*, 26, 3133–3136. https://doi.org/10.1029/1999gl010478.

Limpasuvan, V. and Hartmann, D.L. (2000) Wave-maintained annular modes of climate variability. *Journal of Climate*, 13, 4414–4429. https://doi.org/10.1175/1520-0442.

Liu, Y. and He, S.P. (2020) Strengthened linkage between November/December North Atlantic Oscillation and subsequent January European precipitation after the late 1980s. *Journal of Climate*, 33, 8281–8300. https://doi.org/10.1175/jcli-d-19-0662.1.

Lu, H., Gray, L.J., Anstey, J.A. and Osprey, S.M. (2020) On the role of Rossby wave breaking in the quasi-biennial modulation of the stratospheric polar vortex during boreal winter. *Quarterly Journal of the Royal Meteorological Society*, 146, 1939–1959.

Luo, D., Zhou, W. and Wei, K. (2010) Dynamics of eddy-driven North Atlantic Oscillations in a localized shifting jet: zonal structure and downstream blocking. *Climate Dynamics*, 34, 73–100. https://doi.org/10.1007/s00382-009-0559-y.

Ma, T., Chen, W., Huangfu, J., Song, L. and Cai, Q. (2021) The observed influence of the Quasi-Biennial Oscillation in the lower equatorial stratosphere on the East Asian winter monsoon during early boreal winter. *International Journal of Climatology*, 41, 6254–6269. https://doi.org/10.1002/joc.7192.

Ma, T.J., Chen, W., Graf, H.F., Ding, S.Y., Xu, P.Q., Song, L. and Lan, X.Q. (2020) Different impacts of the East Asian winter monsoon on the surface air temperature in North America during ENSO and neutral ENSO years. *Journal of Climate*, 33, 10671–10690. https://doi.org/10.1175/Jcli-D-18-0760.1.

Marshall, A.G. and Scaife, A.A. (2009) Impact of the QBO on surface winter climate. *Journal of Geophysical Research-Atmospheres*, 114, 6. https://doi.org/10.1029/2009jd011737.

Naito, Y. and Hirota, I. (1997). Interannual variability of the northern winter stratospheric circulation related to the qbo and the solar cycle. *journal of the meteorological society of japan. Ser. II*, 75(4), 925–937. https://doi.org/10.2151/jmsj1965.75.4_925

Nie, Y., Ren, H.L. and Zhang, Y. (2019b) The role of extratropical air–sea interaction in the autumn subseasonal variability of the North Atlantic Oscillation. *Journal of Climate*, 32, 7697–7712. https://doi.org/10.1175/Jcli-D-19-0060.1.

Nie, Y., Scaife, A.A., Li Ren, H., Comer, R.E., Andrews, M.B., Davis, P. and Martin, N. (2019a) Stratospheric initial conditions provide seasonal predictability of the North Atlantic and Arctic Oscillations. *Environmental Research Letters*, 14, 034006. https://doi.org/10.1088/1748-9326/ab0385.

Ning, L. and Bradley, R.S. (2016) NAO and PNA influences on winter temperature and precipitation over the eastern United States in CMIP5 GCMs. *Climate Dynamics*, 46, 1257–1276. https://doi.org/10.1007/s00382-015-2643-9.

Nishimoto, E. and Yoden, S. (2017) Influence of the stratospheric Quasi-Biennial Oscillation on the Madden–Julian Oscillation during austral summer. *Journal of the Atmospheric Sciences*, 74, 1105–1125. https://doi.org/10.1175/Jas-D-16-0205.1.

Ogi, M., Tachibana, Y. and Yamazaki, K. (2003) Impact of the wintertime North Atlantic Oscillation (NAO) on the summertime atmospheric circulation. *Geophysical Research Letters*, 30, 1704. https://doi.org/10.1029/2003gl017280.

Perlwitz, J. and Graf, H.F. (2001) Troposphere–stratosphere dynamic coupling under strong and weak polar vortex conditions. *Geophysical Research Letters*, 28, 271–274. https://doi.org/10.1029/2000gl012405.

Qiao, S.B. and Feng, G.L. (2016) Impact of the December North Atlantic Oscillation on the following February East Asian trough. *Journal of Geophysical Research: Atmospheres*, 121, 10074–10088. https://doi.org/10.1002/2016jd025007.

Rao, J., Garfinkel, C.I. and White, I.P. (2020) How does the Quasi-Biennial Oscillation affect the boreal winter tropospheric circulation in CMIP5/6 models? *Journal of Climate*, 33, 8975–8996. https://doi.org/10.1175/jcli-d-20-0024.1.

Rayner, N.A., Parker, D.E., Horton, E.B., Folland, C.K., Alexander, L.V., Rowell, D.P., Kent, E.C. and Kaplan, A. (2003) Global analyses of sea surface temperature, sea ice, and night marine air temperature since the late nineteenth century. *Journal of Geophysical Research: Atmospheres*, 108, 4407. https://doi.org/10.1029/2002jd002670.

Riviere, G. and Orlanski, I. (2007) Characteristics of the Atlantic storm-track eddy activity and its relation with the North Atlantic Oscillation. *Journal of the Atmospheric Sciences*, 64, 241–266. https://doi.org/10.1175/jas3850.1.

Rogers, J.C. (1997) North Atlantic storm track variability and its association to the North Atlantic oscillation and climate variability of northern Europe. *Journal of Climate*, 10, 1635–1647. https://doi.org/10.1175/1520-0442.

Scaife, A.A., Athanassiadou, M., Andrews, M., Arribas, A., Baldwin, M., Dunstone, N., Knight, J., MacLachlan, C., Manzini, E., Müller, W.A., Pohlmann, H., Smith, D., Stockdale, T. and Williams, A. (2014) Predictability of the Quasi-Biennial Oscillation and its northern winter teleconnection on seasonal to decadal timescales. *Geophysical Research Letters*, 41, 1752–1758. https://doi.org/10.1002/2013GL059160.

Scaife, A.A., Knight, J.R., Vallis, G.K. and Folland, C.K. (2005) A stratospheric influence on the winter NAO and North Atlantic surface climate. *Geophysical Research Letters*, 32, L18715. https://doi.org/10.1029/2005gl023226.

Song, L. and Wu, R.G. (2020) Modulation of the QBO on the MJO-related surface air temperature anomalies over Eurasia during boreal winter. *Climate Dynamics*, 54, 2419–2431. https://doi.org/10.1007/s00382-020-05122-8.

Song, Y.C. and Robinson, W.A. (2004) Dynamical mechanisms for stratospheric influences on the troposphere. *Journal of the Atmospheric Sciences*, 61, 1711–1725. https://doi.org/10.1175/1520-0469.

Thompson, D.W.J. and Wallace, J.M. (2000). Annular Modes in the Extratropical Circulation. Part I: Month-to-Month Variability*. *Journal of Climate*, 13(5), 1000–1016. https://doi.org/10.1175/1520-0442(2000)013<1000:amitec>2.0.co;2

Vallis, G.K. (2017) *Atmospheric and Oceanic Fluid Dynamics*. Cambridge: Cambridge University Press.

Walter, K. and Graf, H.F. (2005) The North Atlantic variability structure, storm tracks, and precipitation depending on the polar vortex strength. *Atmospheric Chemistry and Physics*, 5, 239–248. https://doi.org/10.5194/acp-5-239-2005.

Wanner, H., Bronnimann, S., Casty, C., Gyalistras, D., Luterbacher, J., Schmutz, C., Stephenson, D.B. and Xoplaki, E. (2001) North Atlantic Oscillation—concepts and studies. *Surveys in Geophysics*, 22, 321–382. https://doi.org/10.1023/a:1014217317898.

Wei, K., Chen, W. and Huang, R. (2007) Association of tropical Pacific sea surface temperatures with the stratospheric Holton-Tan Oscillation in the Northern Hemisphere winter. *Geophysical Research Letters*, 34, L16814. https://doi.org/10.1029/2007gl030478.

Wibig, J. (1999) Precipitation in Europe in relation to circulation patterns at the 500 hPa level. *International Journal of Climatology*, 19, 253–269. https://doi.org/10.1002/(sici)1097-0088.

Wu, R. and Chen, S. (2020) What leads to persisting surface air temperature anomalies from winter to following spring over mid- to high-latitude Eurasia? *Journal of Climate*, 33, 5861–5883. https://doi.org/10.1175/jcli-d-19-0819.1.

Xie, F., Li, J., Zhang, J., Tian, W., Hu, Y., Zhao, S., Sun, C., Ding, R., Feng, J. and Yang, Y. (2017) Variations in North Pacific sea surface temperature caused by Arctic stratospheric ozone anomalies. *Environmental Research Letters*, 12, 114023.

Xue, X., Chen, W., Chen, S. and Zhou, D. (2015) Modulation of the connection between boreal winter ENSO and the South Asian High in the following summer by the stratospheric Quasi-Biennial Oscillation. *Journal of Geophysical Research: Atmospheres*, 120, 7393–7411.

Yin, J.H. (2005) A consistent poleward shift of the storm tracks in simulations of 21st century climate. *Geophysical Research Letters*, 32, L18701. https://doi.org/10.1029/2005gl023684.

Zhang, J.K., Xie, F., Ma, Z.C., Zhang, C.Y., Xu, M., Wang, T. and Zhang, R.H. (2019) Seasonal evolution of the Quasi-Biennial Oscillation impact on the Northern Hemisphere polar vortex in winter. *Journal of Geophysical Research: Atmospheres*, 124, 12568–12586. https://doi.org/10.1029/2019jd030966.

Zhang, R.H., Tian, W.S. and Wang, T. (2020) Role of the Quasi-Biennial Oscillation in the downward extension of stratospheric northern annular mode anomalies. *Climate Dynamics*, 55, 595–612. https://doi.org/10.1007/s00382-020-05285-4.

How to cite this article: Cai, Q., Ma, T., Chen, W., Wei, K., Pogoreltsev, A. I., & Koval, A. V. (2022). The observed connection between the Quasi-Biennial Oscillation and the persistence of the North Atlantic Oscillation in boreal winter. *International Journal of Climatology*, 1–15. https://doi.org/10.1002/joc.7769